

Relationships Between the $\Sigma 9$ and $\Sigma 27$ Boundaries and the Connectivity of Random Boundary in Hastelloy C-276 Alloy

Zhang Xiaoyu^{1,2}, Zhao Xianming¹, Li Defu², Guo Shengli²

¹ State Key Laboratory of Rolling and Automation, Northeastern University, Shenyang 110819, China; ² Beijing General Research Institute for Nonferrous Metals, Beijing 100088, China

Abstract: Hastelloy C-276 was subjected to 10% deformation and annealed at 1100 °C for different time. The fractions of $\Sigma 3^n$ ($n=1, 2, 3$) boundaries and the connectivity of random boundary networks were characterized by electron back-scatter diffraction (EBSD). The results show that the $\Sigma 3$ boundary fraction is hardly increased during the annealing period. Instead, the fractions of $\Sigma 9$ and $\Sigma 27$ boundaries have a dramatic change with annealing time, whose peaks are arisen after annealing for 15 min. Meanwhile, the corresponding connectivity of random boundary network is effectively disrupted. This can be attributed to the incoherent $\Sigma 3$ boundary producing more $\Sigma 9$ and $\Sigma 27$ boundaries and incorporating those boundaries into the random boundary networks. Actually, the connectivity of random boundary networks can be definitely identified by $\Sigma(9+27)/\Sigma 3$ ratio.

Key words: Hastelloy C-276 alloy; $\Sigma 9$ and $\Sigma 27$ boundary; connectivity of random boundary network; EBSD

Hastelloy C-276 alloy is a nickel-based alloy with high concentrations of Cr and Mo, which has been widespread used in the chemical, aerospace and nuclear industry^[1-3]. This is attributed to its good mechanical and physical properties and resistance to a wide variety of corrosive environments. However, intergranular corrosion is still a serious problem for Hastelloy C-276 exposed to aggressive environments, due to the grain boundary precipitation of M_6C and the formation of Mo depletion regions^[4,5]. It can cause serious intergranular corrosion. In order to improve the resistance of intergranular failure, grain boundary engineering has been proved to be a good method.

In recent years, the studies on the effect of grain boundary structure on intergranular corrosion were reported^[6-8]. These results showed that the morphology of carbides precipitated at different grain boundaries were widely various. Hence, the different grain boundaries have various abilities to resist intergranular corrosion. The low Σ coincidence site lattice (CSL) boundaries can be proved to have a great resistance to intergranular corrosion^[6,9].

The grain boundary engineering (GBE) concept was first proposed by Watanabe in the early 1980s^[10]. Its goal is to

increase the frequency of low Σ CSL boundaries ($\Sigma \leq 29$), so-called special boundaries, by thermos-mechanical treatments for enhancing the grain-boundary related properties of materials. The thermos-mechanical treatments include two processing paths: one is carried out at low levels of strain followed by long annealing time^[11,12]. The other is employed by moderate levels of stain with short anneals^[13,14].

In this work, the goal of understanding the effect of annealing time on the $\Sigma 9$ and $\Sigma 27$ factions was investigated, and the relationship between $\Sigma(9+27)/\Sigma 3$ ratio and the connectivity of random boundary was revealed.

1 Experiment

Hastelloy C-276 sheet with 1 mm in diameter was used in study whose chemical composition (wt%) is 15.07 Cr, 15.53 Mo, 4.14 Fe, 4.04 W, 2.5 Co, 0.62 Mn, 0.01 P, 0.08 Si, 0.012 C, 0.002 S and Bal Ni. The samples were solution annealed at a temperature of 1100 °C for 15 min followed by water quenching. After that, those solution annealed samples were subjected to cold-rolling 10% in the thickness direction, and then annealed at 1100 °C for 5, 15, 30 and 60 min.

The samples were mechanically polished, and then electro-

polished in an electrolyte containing $\text{H}_2\text{SO}_4:\text{CH}_3\text{COOH}=1:4$ at room temperature. The fractions of special boundaries were determined by electron backscatter diffraction (EBSD) using a JEOL JSM7001LV SEM with EDAX (TSL) OIM Data Collection 6.0 software. The step size was chosen to be $2\ \mu\text{m}$ for scanning. The Brandon Criterion^[15] was used to classify coincidence site lattice (CSL) boundaries, as a fraction of total boundary length. Those boundaries with $\Sigma \leq 29$ were considered special boundaries, using 2° as a minimum disorientation for a low-angle boundary.

2 Results

2.1 Fraction of $\Sigma 3$ boundary

The $\Sigma 3$ boundary is known as the annealing twin boundary that is characterized as 60° rotation with respect to the $\langle 111 \rangle$ axis. It can be regarded as the main element of GBE. The effect of annealing time on the fraction of $\Sigma 3$ boundary for 10% strain samples is shown in Fig.1. It is shown that the fraction of $\Sigma 3$ boundary is around 51%, which is not increased obviously. It indicates that the annealing time has little effect on the fraction of $\Sigma 3$ boundary. Instead, the strain could play an important role in the variety of $\Sigma 3$ boundary.

2.2 Fractions of $\Sigma 9$ boundary and $\Sigma 27$ boundary

The relationships of $\Sigma 9$ and $\Sigma 27$ boundaries values to annealing time are shown in Fig.2. It can be seen that the fraction of $\Sigma 9$ boundary is firstly increased as annealing time is prolonged from 5 min to 15 min. Its peak value reaches 4%. Then $\Sigma 9$ boundary fraction is decreased drastically with annealing time prolonged from 15 min to 60 min. Similarly, the fraction of $\Sigma 27$ boundary has the same tendency with $\Sigma 9$ boundary. Its maximum value is also arisen at 15 min, up to 1.7%. It can be found that the effect of annealing time on the fractions of $\Sigma 9$ and $\Sigma 27$ boundaries is very obvious. Therefore, the reasonable annealing time contributes to the generation the $\Sigma 9$ and $\Sigma 27$ boundaries.

2.3 Radios of $\Sigma(9+27)/\Sigma 3$ during annealing

The values of $\Sigma(9+27)/\Sigma 3$ radio as a function of annealing time are shown in Fig.3. With annealing time prolonged, the

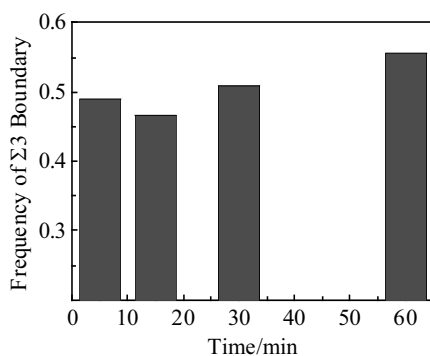


Fig.1 Effect of annealing time at $1100\ ^\circ\text{C}$ on the fraction of $\Sigma 3$ boundary

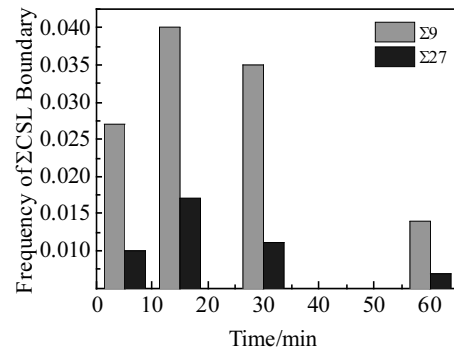


Fig.2 Relationships between $\Sigma 9$ and $\Sigma 27$ boundaries fractions and annealing time

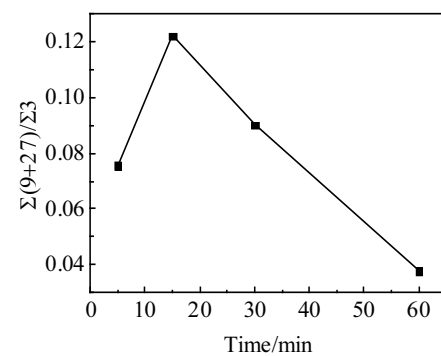


Fig.3 Values of $\Sigma(9+27)/\Sigma 3$ radio as a function of annealing time

$\Sigma(9+27)/\Sigma 3$ radio is firstly increased and then dramatically decreased. When annealed for 15 min, it is up to the peak value, 0.122. The $\Sigma(9+27)/\Sigma 3$ radio demonstrates a trend similar to $\Sigma 9$ and $\Sigma 27$ boundaries variations. As the research^[16,17] reported, it can indicate the interactions of $\Sigma 3^n$ boundaries.

2.4 Connectivity of random boundary network during annealing

Fig.4 shows the random boundary network maps where special boundaries are shown in grey and random boundaries in black. It will be qualitative to see if the special grain boundary and distribution can break up the random boundary connectivity. In Fig.4, it is seen that the random boundary networks are effectively disrupted by special boundary when annealed for 15 min, whereas other samples remain integrity. The dramatic contrasts between those samples may be attributed to the different $\Sigma 9$ and $\Sigma 27$ boundaries values. This suggests that there is a clear relationship between $\Sigma 9$ and $\Sigma 27$ boundary fractions and random boundary connectivity.

3 Discussions

Random boundaries are believed to be more susceptible to creep^[18,19], intergranular corrosion^[6-9], and crack propagation^[20,21] than special boundaries. By disrupting their connectivity, it may be possible to prevent from propagating

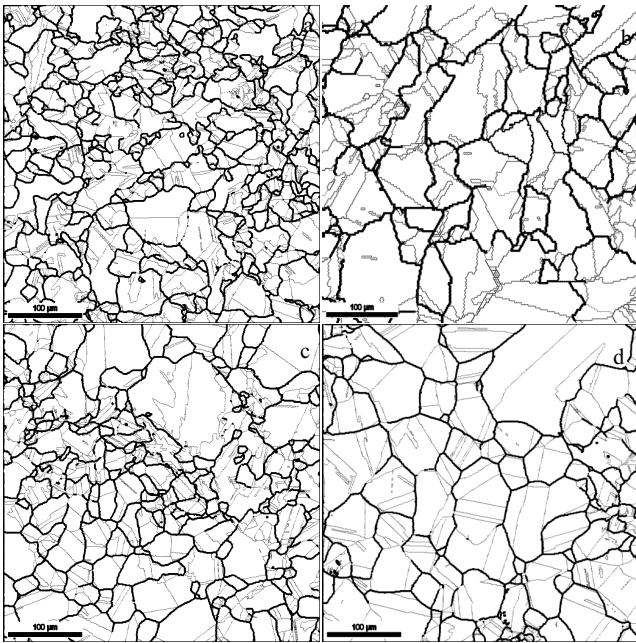


Fig.4 Maps of connectivity of random boundary networks of 10% strain sample annealed at 1100 °C for various time: (a) 5 min, (b) 15 min, (c) 30 min, and (d) 60 min (the black and gray lines indicate random and special boundaries, respectively)

cracks and intergranular corrosion attack at special boundary junctions.

As expected after GBE-type processing, a high proportion of $\Sigma 3$ boundaries is evident in the microstructure, colored red lines as shown in Fig.5. Correspondingly, the $\Sigma 3$ proportions after sing-step processing are shown in Fig.1. The $\Sigma 9$ and $\Sigma 27$ boundary fractions are also included In Fig.2. The proportion of $\Sigma 3$ boundary increases slightly after annealed at 1100 °C from 5 min to 60 min. However, the $\Sigma 9$ proportions have changed significantly during the same annealing time. Likewise, the variation of $\Sigma 27$ proportion is also dramatic. The $\Sigma(9+27)/\Sigma 3$ ratio is also peaking at the same annealing time.

Comparison of the $\Sigma(9+27)/\Sigma 3$ ratios and connectivity of random boundaries changes reveals an interesting relationship that the $\Sigma(9+27)/\Sigma 3$ ratio can really reflect the connectivity of random boundaries. Higher $\Sigma(9+27)/\Sigma 3$ ratio can enhance the reduction of connectivity, which can be observed in Fig.3 and Fig.4. It is reasonable to assume that random boundary connectivity should be increasingly disrupted by increasing $\Sigma 9$ and $\Sigma 27$ boundaries.

It can be seen from Fig.4, that the random boundary network has been disrupted by special boundaries. However, the connectivity of random boundary networks in annealed 5, 30 and 60 min samples is less interrupted than the annealed 15 min sample. Although the values of $\Sigma 3$ boundary fraction are nearly the same as annealing time extended from 5 min to 60 min in Fig.1, the values of $\Sigma 9$ and $\Sigma 27$ boundary fractions are

obviously different. The peaks of $\Sigma 9$ and $\Sigma 27$ appear at 15 min, which suggest that the interaction of $\Sigma 3^n$ boundaries should be active. A higher ratio of $\Sigma(9+27)/\Sigma 3$ means the $\Sigma 3$ regeneration mechanism. This is due to the interactions of $\Sigma 3^n$ boundaries, which could incorporate the $\Sigma 3^n$ boundaries into the random boundary networks. On the other hand, lower ratio of $\Sigma(9+27)/\Sigma 3$ defines poor interruption of random boundary networks. It also means that the new twinning formation is more active than $\Sigma 3$ regeneration mechanism, which cannot have an effect on the random boundary networks.

The OIM maps of samples annealed at 1100 °C for various time are shown in Fig.5. The appearance and distribution of $\Sigma 3$ boundaries are quite different in Fig.5b and 5d. Some of $\Sigma 3$ boundaries with a little curvature, are generally located in Fig.5b. According the sing-section trace analysis^[22,23], those $\Sigma 3$ boundaries are identified as incoherent twin boundaries. On the contrary, in Fig.5a, 5b and 5d, the main boundaries are $\Sigma 3$ boundaries, most of which in these maps are in the shape of a straight single line or parallel line pairs within grains. So the $\Sigma 3$ boundaries are coherent twin boundaries by the technique of single-section trace. In the investigations^[24,25], the incoherent $\Sigma 3$ boundaries will migrate and interact with other special boundaries to produce more $\Sigma 9$ and $\Sigma 27$ boundaries, which can be evidenced in Fig.2 and the visual break-up in the connectivity of random boundary networks in Fig.4b. It also reveals that the incoherent twin boundaries contribute to disrupting the connectivity of random boundary network.

The formation of twin-induced $\Sigma 3$ boundaries could effectively interrupt the connectivity of the random boundary

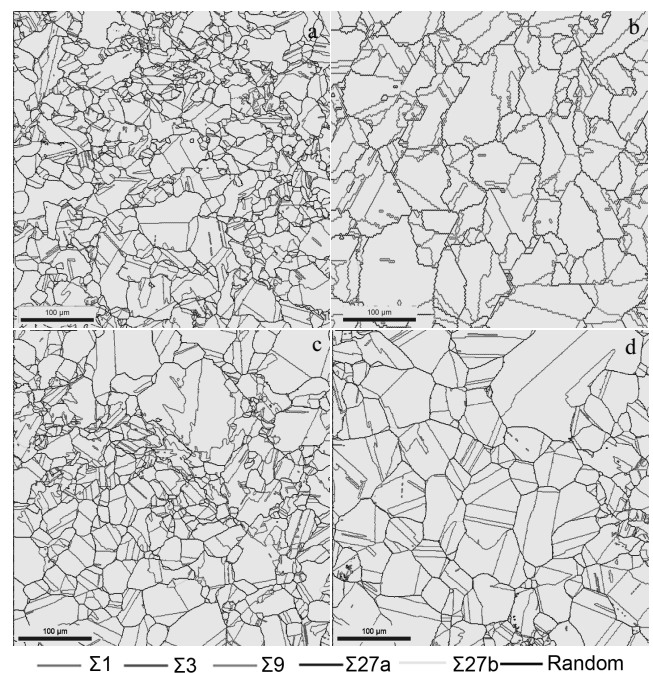


Fig.5 OIM maps of map of 10% strain sample annealed at 1100 °C for various time: (a) 5 min, (b) 15 min, (c) 30 min, and (d) 60 min

networks, which can enhance the resistance to intergranular failure of the Hastelloy C-276 alloy by rational annealing treatment. It is helpful to applying the GBE processing to the manufacturing of products.

4 Conclusions

1) The fractions of $\Sigma 9$ and $\Sigma 27$ boundaries and the corresponding connectivity of random boundary networks are observed in 10% strain sample annealed at 1100 °C for different time.

2) The $\Sigma 3$ boundary fraction is hardly increased, while the fractions of $\Sigma 9$ and $\Sigma 27$ boundaries have a dramatic change with the annealing time, their peaks are simultaneously arisen when annealed for 15 min.

3) The connectivity of random boundary networks is disrupted by the increasing of $\Sigma 9$ and $\Sigma 27$ boundaries, which is attributed to the existence of incoherent $\Sigma 3$ boundaries. However, the $\Sigma(9+27)/\Sigma 3$ ratio can well define the connectivity of random boundary networks.

References

- Zhang Q, Tang R, Yin K et al. *Corrosion Science*[J], 2009, 51(9): 2092
- Akhter J I, Shaikh M A, Ahmad M et al. *Journal of Materials Science Letters*[J], 2001, 20(4): 333
- Lu Y, Liu J, Li X et al. *Transactions of Nonferrous Metals Society of China*[J], 2012, 22: 84
- Tawancy H M. *Journal of Materials Science*[J], 1981, 16(10): 2883
- Raghavan M, Berkowitz B J, Scanlon J C. *Metallurgical Transactions A*[J], 1982, 13(6): 979
- Hu C, Xia S, Li H et al. *Corrosion Science*[J], 2011, 53(5): 1880
- Li H, Xia S, Zhou B et al. *Journal of Nuclear Materials*[J], 2010, 399(1): 108
- Shi F, Tian P C, Jia N et al. *Corrosion Science*[J], 2016, 107: 49
- West E A, Was G S. *Journal of Nuclear Materials*[J], 2009, 392(2): 264
- Watanabe T. *Res Mechanica*[J], 1984, 11(1): 47
- Li Q, Guyot B M, Richards N L. *Materials Science and Engineering A*[J], 2007, 458(1): 58
- Tan L, Sridharan K, Allen T R. *Journal of Nuclear Materials*[J], 2007, 371(1): 171
- Pinto A L, da Costa Viana C S, de Almeida L H. *Materials Science and Engineering A*[J], 2007, 445: 14
- Li Q, Cahoon J R, Richards N L. *Materials Science and Engineering A*[J], 2009, 527(1): 263
- Brandon D G. *Acta Metall*[J], 1966, 14: 1479
- Akhiani H, Nezakat M, Sanayei M et al. *Materials Science and Engineering A*[J], 2015, 626: 51
- Randle V, Owen G. *Acta Materialia*[J], 2006, 54(7): 1777
- Thaveprungsriporn V, Was G S. *Metallurgical and Materials Transactions*[J], 1997, 28(10): 2101
- Spigarelli S, Cabibbo M, Evangelista E et al. *Materials Science and Engineering A*[J], 2003, 352(1): 93
- Krupp U, Kane W M, Liu X et al. *Materials Science and Engineering A*[J], 2003, 349(1): 213
- Jin Y J, Lu H, Yu C et al. *Materials Characterization*[J], 2013, 84: 216
- Randle V. *Scripta Materialia*[J], 2001, 44(12): 2789
- Wright S I, Larsen R J. *Journal of Microscopy*[J], 2002, 205(3): 245
- Fang X, Zhang K, Guo H et al. *Materials Science and Engineering A*[J], 2008, 487(1): 7
- Wang W, Yin F, Guo H et al. *Materials Science and Engineering A*[J], 2008, 491(1): 199

Hastelloy C-276 合金中 $\Sigma 9$ 和 $\Sigma 27$ 晶界与随机晶界网络连通性的关系

张晓宇^{1,2}, 赵宪明¹, 李德富², 郭胜利²

(1. 东北大学 轧制技术及连轧自动化国家重点实验室, 辽宁 沈阳 110819)

(2. 北京有色金属研究总院, 北京 100088)

摘要: Hastelloy C-276 合金经冷轧 10% 后进行 1100 °C 不同时间的退火热处理。采用 EBSD 技术对 $\Sigma 3^n$ 晶界 ($n=1, 2, 3$) 晶界比例进行统计并对随机晶界网络连通性进行表征。结果表明, 随着退火时间的延长, $\Sigma 3$ 晶界比例基本保持不变, 而 $\Sigma 9$ 和 $\Sigma 27$ 晶界比例却出现较大幅度的变化, 并且其峰值点都出现在退火 15 min 条件下。此刻, 相应的随机晶界网络连通性被有效阻断。这是由于非共格 $\Sigma 3$ 晶界的存在, 产生了更多的 $\Sigma 9$ 和 $\Sigma 27$ 晶界, 并且使得这些特殊晶界连接到随机晶界网络当中。而采用 $\Sigma(9+27)/\Sigma 3$ 比值可以更好的表征随机晶界网络的连通性。

关键词: Hastelloy C-276 合金; $\Sigma 9$ 和 $\Sigma 27$ 晶界; 随机晶界网络; EBSD

作者简介: 张晓宇, 男, 1985 年生, 博士, 北京有色金属研究总院复合材料中心, 北京 100088, E-mail: xy12152006@126.com